Engineered Myosin VI Motors Reveal Minimal Structural Determinants of Directionality and Processivity

5 AUTHORS, INCLUDING:

Jung-Chi Liao
Academia Sinica

34 PUBLICATIONS **387** CITATIONS

SEE PROFILE

Mary Williard Elting
University of California, San Francisco

9 PUBLICATIONS **105** CITATIONS

SEE PROFILE

Scott L Delp
Stanford University

285 PUBLICATIONS **11,239** CITATIONS

SEE PROFILE

James A Spudich
Stanford University

263 PUBLICATIONS **21,647** CITATIONS

SEE PROFILE

JMB

Available online at www.sciencedirect.com

ScienceDirect

ELSEVIER

COMMUNICATION

Engineered Myosin VI Motors Reveal Minimal Structural Determinants of Directionality and Processivity

Jung-Chi Liao[1,2], Mary Williard Elting[2,3], Scott L. Delp[1], James A. Spudich[2] and Zev Bryant[1,2,4]*

[1]*Department of Bioengineering, Stanford University, Stanford, CA 94305, USA*

[2]*Department of Biochemistry, Stanford University Medical Center, Stanford, CA 94305, USA*

[3]*Department of Applied Physics, Stanford University, Stanford, CA 94305, USA*

[4]*Department of Structural Biology, Stanford University Medical Center, Stanford, CA 94305, USA*

Myosins have diverse mechanical properties reflecting a range of cellular roles. A major challenge is to understand the structural basis for generating novel functions from a common motor core. Myosin VI (M6) is specialized for processive motion toward the (−) end of actin filaments. We have used engineered M6 motors to test and refine the "redirected power stroke" model for (−) end directionality and to explore poorly understood structural requirements for processive stepping. Guided by crystal structures and molecular modeling, we fused artificial lever arms to the catalytic head of M6 at several positions, retaining varying amounts of native structure. We found that an 18-residue α-helical insert is sufficient to reverse the directionality of the motor, with no requirement for any calmodulin light chains. Further, we observed robust processive stepping of motors with artificial lever arms, demonstrating that processivity can arise without optimizing lever arm composition or mechanics.

© 2009 Elsevier Ltd. All rights reserved.

*Corresponding author. E-mail address:
zevry@stanford.edu.

Present address: J.-C. Liao, Department of Mechanical Engineering, Columbia University, New York, NY 10027, USA.

Abbreviations used: M6, myosin VI; MD, molecular dynamics.

Members of the myosin superfamily have acquired specialized mechanical adaptations to perform cellular functions ranging from vesicle transport to muscle contraction. Myosin VI (M6) moves toward the (−) end of the actin filament, in the opposite direction from all other characterized myosins.[1] Additionally, unlike muscle myosin II, individual dimers of M6 can travel processively for many steps before detaching from the filament.[2]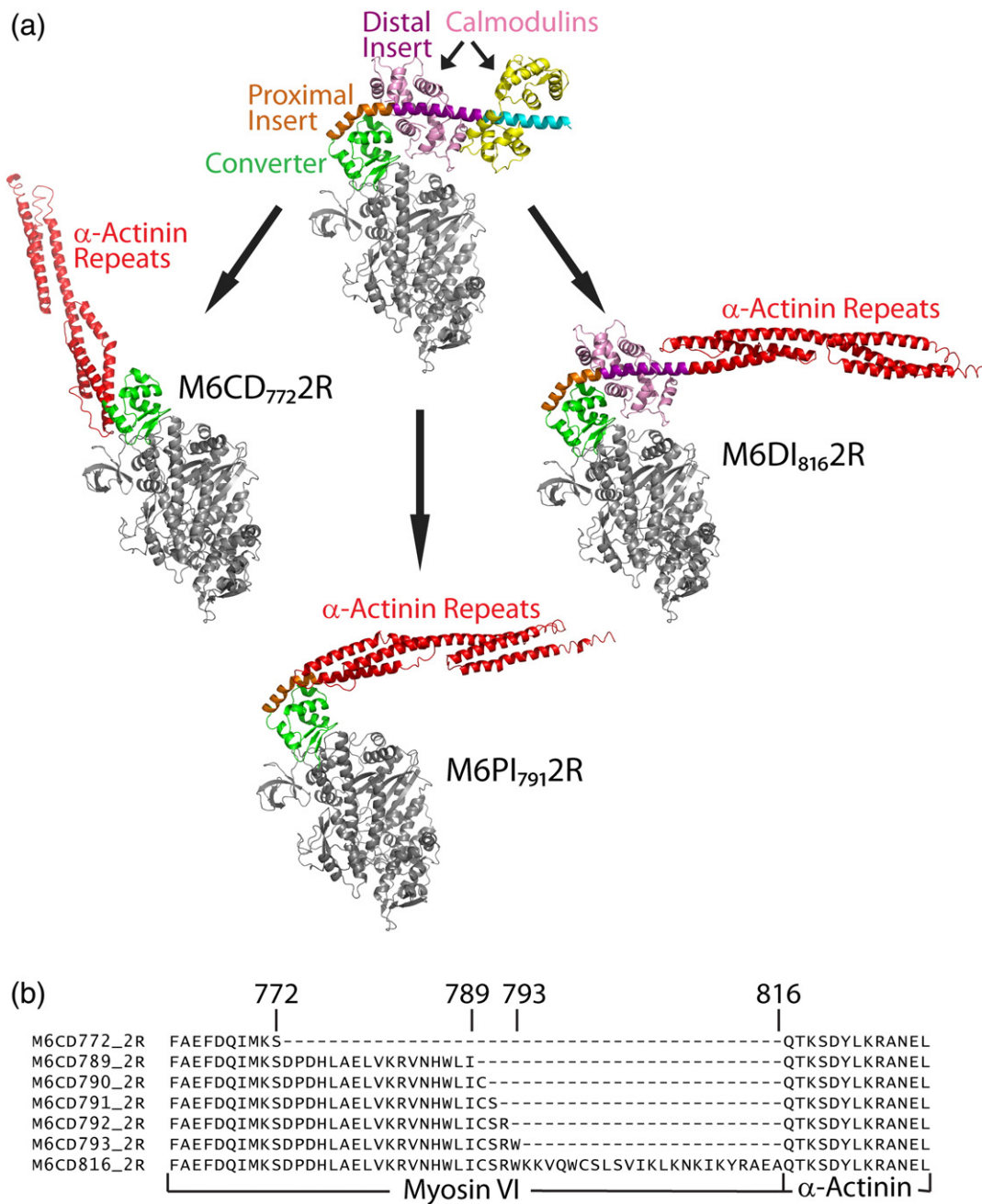 The determinants of M6 directionality and the mechanism of M6 processivity have recently been the subjects of considerable scrutiny.[3–10]

Structural and functional studies have converged on a redirected power stroke model to explain directionality reversal in M6. According to current formulations of the power stroke or swinging cross-bridge model of myosin force generation,[11] conformational changes at the nucleotide binding site are propagated through the catalytic head, driving a large rotation of the converter domain. This rotation is amplified by a rigid lever arm structure extending from the final helix of the converter. An X-ray crystal structure of the M6 post-stroke state showed that the lever arm emerges at an angle that differs from (+) end-directed myosins by ∼120° due to the presence of a unique insert in M6 following the converter (Fig. 1a).[9] Engineered motors truncated before the unique insert show (+) end-directed motion,[3] as do chimeric motors in which M6 is fused immediately after the converter to the lever

Fig. 1. Design of engineered M6 motors. (a) Post-stroke structure of M6 (top) and model structures of chimeric constructs with artificial lever arms derived from α-actinin. In M6CD$_{772}$2R, spectrin repeats from α-actinin are fused after the converter domain but prior to the unique insert; in M6PI$_{791}$2R, the α-actinin repeats are fused immediately after the proximal part of the unique insert; in M6DI$_{816}$2R, the α-actinin repeats are fused after the distal part of the insert. (b) Amino acid sequences of chimeric constructs at the site of fusion between myosin and α-actinin.

arm from myosin V.[5] These studies demonstrate that redirection of the lever arm mediated by the unique insert is essential for (−) end directionality.

An examination of stroke sizes for a series of truncated M6 constructs led to a model in which the redirected lever arm rotates by ∼180° during the power stroke.[3] This model was supported by a subsequent crystal structure of the putative pre-stroke state.[10] However, the pre-stroke crystal structure was obtained using a fragment of M6 that lacks the distal part of the unique insert and its associated

stabilizing light chain. The lever arm angle in this structure could only be deduced by modeling the missing distal insert. The functional relevance of the crystallized conformation, which contains large and surprising rearrangements of the converter domain, must remain tentative in the absence of experiments showing that the proximal part of the unique insert is sufficient to correctly position a lever arm for (−) end-directed motion.

Functional replacement of the myosin II lever arm with rigid three-helix bundles derived from α-actinin

(a)

M6PI$_{791}$2R

(b)

M6PI$_{792}$2R
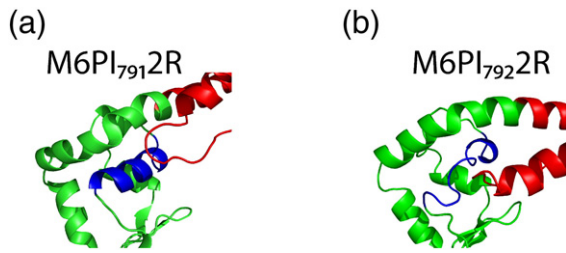
Fig. 2. MD simulations showing predicted differences in stability between alternative proximal insert fusion constructs that differ by one residue in the placement of the fusion point. (a) A snapshot from a simulation of M6PI$_{791}$2R shows stable local structure in the converter domain. (b) A snapshot from a simulation of M6PI$_{792}$2R shows a denatured α-helix (blue) in the converter domain.

provided critical tests of the swinging cross-bridge model for myosin II.[12,13] Here, we have used an extension of this strategy to challenge and refine the redirected power stroke model for M6 directionality. We have characterized M6 constructs in which α-actinin lever arms have been fused at several different locations following the converter domain. We include constructs in which the lever arm is fused immediately following the proximal part of the unique insert, probing whether this structure is sufficient for (−) end directionality.

Our strategy also provides a means to test models relating structure to processivity. Dimers of M6 have been shown to move processively with a hand-over-hand mechanism[8,14] thought to depend on coordination mediated by strain in the lever arms.[15] By replacing lever arms with alternative structural elements, we can directly test the effects on processivity of varying geometric and mechanical parameters in the dimer.

We designed chimeric constructs in which an artificial lever arm[12,16] (two spectrin repeats from *Dictyostelium* α-actinin, designated 2R) was fused to M6 at one of three locations (Fig. 1a and b): (1) after the Converter domain but prior to the unique insert, M6CD$_{772}$2R; (2) immediately after the proximal part of the unique insert, M6PI$_{791}$2R; and (3) after the distal part of the insert, M6DI$_{816}$2R. (Subscripts indicate the residue number of the last native M6 amino acid prior to the 2R junction.) M6CD$_{772}$2R is

predicted to have a lever arm orientation similar to myosin II. The longer constructs are predicted to yield lever arm orientations similar to native M6 but with differences in lever arm stability and mechanics due to the replacement of one or both native calmodulin-binding domains.

Precise fusion points at the level of amino acid residues were chosen with the aid of molecular modeling. For the constructs fused after the proximal part of the unique insert, five possible adjacent fusion points were modeled. Models of M6PI$_{789}$2R and M6PI$_{793}$2R showed steric collisions between the converter and the artificial lever arm. Initial models of M6PI$_{790}$2R, M6PI$_{791}$2R, and M6PI$_{792}$2R were free of structural collisions, but molecular dynamics (MD) simulations for the three models predicted differing stabilities of local structures (Fig. 2 and Supplemental Movies S1 and S2). M6PI$_{790}$2R and M6PI$_{791}$2R remained stable for 5 ns of MD simulation. In contrast, a key α-helix in the converter domain of M6PI$_{792}$2R became disordered during all-atom simulations. Thus, our models predicted that only two of these five fusions should retain functional lever arms: M6PI$_{790}$2R and M6PI$_{791}$2R.

A total of seven monomeric fusion constructs were expressed, purified, and assayed for motility, velocity, and directionality using dual-labeled gliding filament assays. In addition, the dimeric artificial lever arm construct M6DI$_{816}$2RGCN4 was generated by fusion of M6DI$_{816}$2R to the medial tail region of M6 followed by the leucine zipper GCN4 in order to ensure dimerization. This construct was expressed and assayed for processivity using single fluorophore tracking.

Constructs fused after the converter or after the unique insert are motile and have the expected directionalities. M6CD$_{772}$2R shows (+) end-directed motion in dual-labeled gliding filament assays (Fig. 3a and Table 1; Movie S3), consistent with its predicted structural similarity to myosin II. M6DI$_{816}$2R retains the entire unique insert and has an extended lever arm and was thus predicted to show rapid (−) end-directed motion. Assays (Fig. 3b; Movie S4) show the expected movement at an average velocity of −111 nm/s (Table 1), compared with −45 nm/s for a construct truncated after the unique insert alone.[3]

All-atom modeling correctly predicts functional fusion sites. We tested all five constructs fused after the

(a)

M6CD$_{772}$2R

(b)

M6DI$_{816}$2R

(c)

M6PI$_{791}$2R
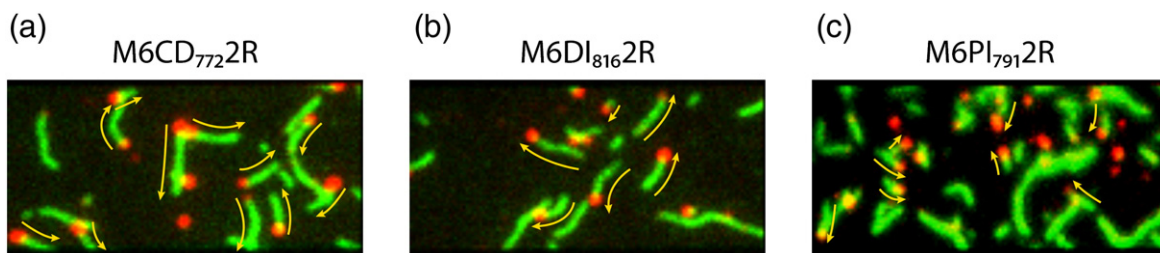
Fig. 3. Images from dual-labeled gliding filament assays showing the directionality of engineered constructs (see also Supplemental Movies S3–S7). Tetramethylrhodamine-phalloidin-labeled actin filaments are false-colored in green; Cy5-labeled (+) ends appear as red dots. The direction of gliding movement is indicated by yellow arrows. (a) M6CD$_{772}$2R shows (+) end-directed movement, while (b) M6DI$_{816}$2R and (c) M6PI$_{791}$2R show (−) end-directed movement.

Table 1. Gliding filament results for engineered M6 motors

|	M6CD$_{772}$2R	M6PI$_{791}$2R	M6DI$_{816}$2R
Directionality	(+) end (51/51 filaments)	(−) end (64/65 filaments)	(−) end (86/89 filaments)
Velocity	+41±2 nm/s ($n=44$)	−29±1 nm/s ($n=32$)	−111±4 nm/s ($n=51$)

proximal part of the unique insert and observed only stationary actin filaments in assays of the three constructs (M6PI$_{789}$2R, M6PI$_{792}$2R, and M6PI$_{793}$2R) showing steric clashes or helix instability in MD simulations (Movie S5). Both of the constructs that remained stable in MD simulations (M6PI$_{790}$2R and M6PI$_{791}$2R) were motile (Movies S6 and S7).

Constructs fused after the proximal part of the unique insert are (−) end directed, showing that the distal part of the insert is dispensable for directionality reversal. M6PI$_{790}$2R and M6PI$_{791}$2R show robust (−) end-directed motion in gliding filament assays (Fig. 3c and Table 1). These constructs move in the opposite direction from M6CD$_{772}$2R due to the insertion of only 18–19 amino acids that form a proline kink and a short α-helical section, without any stabilizing light chains.

Table 1 summarizes gliding filament results for monomeric engineered M6 motors. Directionalities agree with predictions and demonstrate that a short α-helical insert is sufficient to reverse the directionality of the motor. In these assays, polarity-labeled filaments occasionally become mislabeled, likely due to loss of the gelsolin cap on some Cy5-actin seeds.[17] This explains results with M6PI$_{791}$2R and M6DI$_{816}$2R, in which fewer than 100% of filaments were scored as (−) end directed. As expected, the highest gliding filament velocity is seen for M6DI$_{816}$2R, which has the longest lever arm length (Fig. 1). M6CD$_{772}$2R and M6PI$_{791}$2R are expected to have relatively lower velocities due to shortened stroke sizes. Further reductions in velocity for the shortened constructs may occur due to increased actin attachment times, as seen previously for truncated M6 constructs lacking light-chain binding regions.[3]

Artificial lever arms can support processive movement. The dimeric construct M6DI$_{816}$2RGCN4 was tested for processivity and compared to M6-GCN4 control (Fig. 4a and b). We used total internal reflection fluorescence imaging to track the movement of individual tetramethylrhodamine-labeled dimers on actin filaments (Movie S8). M6DI$_{816}$2RGCN4 showed processive movement similar to control
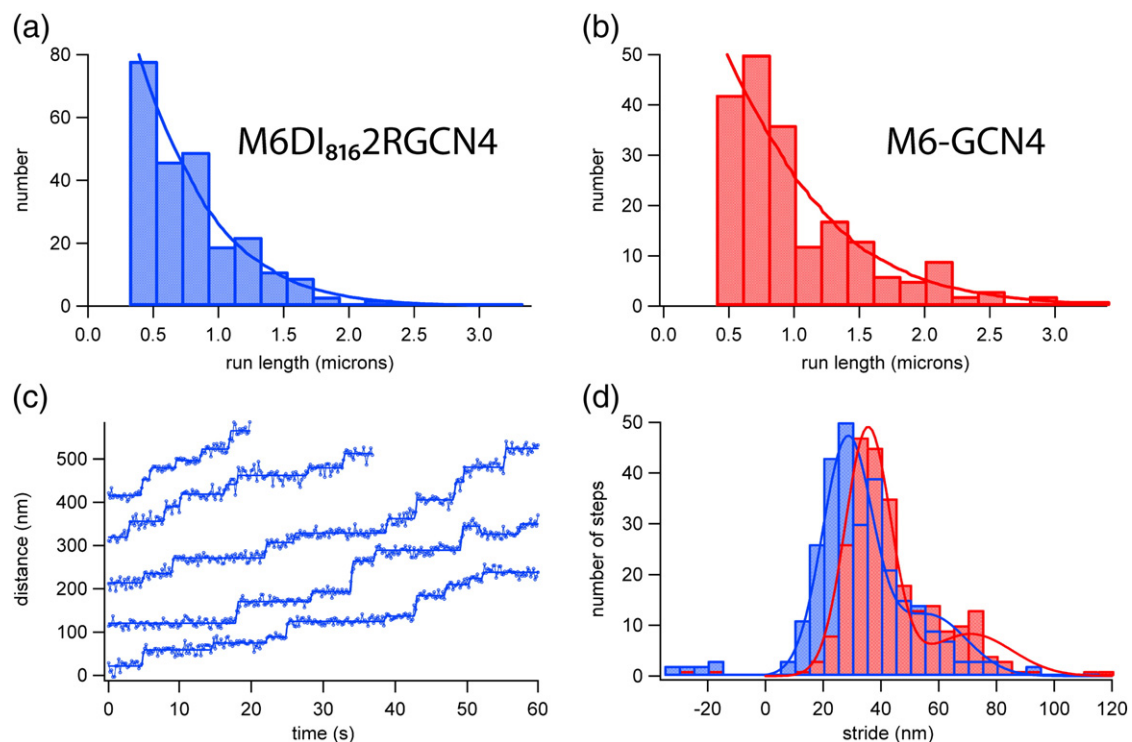
Fig. 4. Processive data from single-fluorophore tracking of tetramethylrhodamine-labeled dimeric constructs. (a and b) Histograms of processive run lengths for a dimeric M6 with artificial lever arms, M6DI$_{816}$2RGCN4 (mean run length, 590±50 nm; $n=243$) and control M6-GCN4 (854±91 nm; $n=199$). (c) Sample stepping traces for M6DI$_{816}$2RGCN4. Blue circles, data from fluorophore localization; solid blue lines, step-finding fits. (d) Stride histograms show that M6DI$_{816}$2RGCN4 (blue) has a slightly shorter stride (28.4±0.5 nm) than M6-GCN4 (red) (35.5±0.5 nm).

dimeric M6-GCN4, with run lengths approximately 70% as long as those of the control. Stepwise motion was detected during processive runs for both M6-GCN4 and M6DI$_{816}$2RGCN4 (Fig. 4c), allowing us to measure the distribution of stride sizes (Fig. 4d). As expected from the extended lever arm design, M6DI$_{816}$2RGCN4 stepped along the actin filament with long strides (28.4±0.5 nm). However, the peak stride size for M6DI$_{816}$2RGCN4 was significantly smaller than that for control M6-GCN4 (35.5±0.5 nm), reflecting differences in lever arm geometry.

Directionality reversal in M6 was previously shown to depend on the presence of the 50-residue unique insert and its associated calmodulin light chain.[3,5] This light chain makes extensive contacts with the converter domain in the native M6 structure, suggesting that it might play an important structural role in redirection of the lever arm.[9] However, we have shown here that the light chain and the distal part of the unique insert are dispensable for directionality reversal. Our results help validate the interpretation of a pre-stroke crystal structure for M6 in which the lever arm angle was assumed to be unperturbed by omission of the distal part of the unique insert and its associated light chain.[10] This provides additional support for a model in which the M6 lever arm is nearly perpendicular to the actin filament and rotates close to 180° during the power stroke.[3,9,10,18]

We have also shown that processive motion can be achieved in a dimeric myosin using artificial lever arms and without extensive optimization of lever arm geometry or mechanics. (Lack of geometric optimization in our constructs is underscored by the significantly shorter stride of the chimera, which fails to match the actin pseudo-repeat.) In most models of hand-over-hand motion, coordination of the two myosin heads is hypothesized to depend on internal strain generated when both heads are bound to the actin filament.[15,19] The mechanical properties of the lever arms might therefore be tuned for strain-mediated communication between the heads, and the lever arms might also be optimized for thermally sampling conformations during the binding site search that precedes front head reattachment. Computational models have led researchers to propose stringent mechanical requirements for lever arms: Lan and Sun found that bending anisotropy was a key feature of computational models for myosin V stepping.[20] Our findings imply that either coordination is robust to changes in lever arm composition or else coordination is relatively unimportant for processive motion. Indeed, as previously suggested,[19] dimers with independently cycling heads may theoretically be expected to show substantial processive motion, as long as the duty ratio of each monomer is high.

Finally, we note that while chimeric proteins can be powerful tools for structure/function studies, they must fold correctly in order to provide useful information. Here, we used all-atom molecular modeling to predict misfolding at junctions due to steric clashes or other unfavorable interactions. We found that relatively simple atomistic computations helped discriminate between functional and non-functional chimeras. For chimeras involving extensive new domain interfaces, it may be necessary to apply sequence selection by structure-based protein design, as demonstrated earlier for a homing endonuclease.[21]

Supplementary Data

Supplementary data associated with this article can be found, in the online version, at doi:10.1016/j.jmb.2009.07.046

References

1. Wells, A. L., Lin, A. W., Chen, L. Q., Safer, D., Cain, S. M., Hasson, T. *et al.* (1999). Myosin VI is an actin-based motor that moves backwards. *Nature*, **401**, 505–508.
2. Rock, R. S., Rice, S. E., Wells, A. L., Purcell, T. J., Spudich, J. A. & Sweeney, H. L. (2001). Myosin VI is a processive motor with a large step size. *Proc. Natl Acad. Sci. USA*, **98**, 13655–13659.
3. Bryant, Z., Altman, D. & Spudich, J. A. (2007). The power stroke of myosin VI and the basis of reverse directionality. *Proc. Natl Acad. Sci. USA*, **104**, 772–777.
4. Iwaki, M., Tanaka, H., Iwane, A. H., Katayama, E., Ikebe, M. & Yanagida, T. (2006). Cargo-binding makes a wild-type single-headed myosin-VI move processively. *Biophys. J.* **90**, 3643–3652.
5. Park, H., Li, A., Chen, L. Q., Houdusse, A., Selvin, P. R. & Sweeney, H. L. (2007). The unique insert at the end of the myosin VI motor is the sole determinant of directionality. *Proc. Natl Acad. Sci. USA*, **104**, 778–783.
6. Park, H., Ramamurthy, B., Travaglia, M., Safer, D., Chen, L. Q., Franzini-Armstrong, C. *et al.* (2006). Full-length myosin VI dimerizes and moves processively along actin filaments upon monomer clustering. *Mol. Cell*, **21**, 331–336.
7. Rock, R. S., Ramamurthy, B., Dunn, A. R., Beccafico, S., Rami, B. R., Morris, C. *et al.* (2005). A flexible domain is essential for the large step size and processivity of myosin VI. *Mol. Cell*, **17**, 603–609.
8. Yildiz, A., Park, H., Safer, D., Yang, Z., Chen, L. Q., Selvin, P. R. & Sweeney, H. L. (2004). Myosin VI steps

via a hand-over-hand mechanism with its lever arm undergoing fluctuations when attached to actin. *J. Biol. Chem.* **279**, 37223–37226.

9. Menetrey, J., Bahloul, A., Wells, A. L., Yengo, C. M., Morris, C. A., Sweeney, H. L. & Houdusse, A. (2005). The structure of the myosin VI motor reveals the mechanism of directionality reversal. *Nature*, **435**, 779–785.

10. Menetrey, J., Llinas, P., Mukherjea, M., Sweeney, H. L. & Houdusse, A. (2007). The structural basis for the large powerstroke of myosin VI. *Cell*, **131**, 300–308.

11. Holmes, K. C., Schroder, R. R., Sweeney, H. L. & Houdusse, A. (2004). The structure of the rigor complex and its implications for the power stroke. *Philos. Trans. R. Soc. London, Ser. B*, **359**, 1819–1828.

12. Anson, M., Geeves, M. A., Kurzawa, S. E. & Manstein, D. J. (1996). Myosin motors with artificial lever arms. *EMBO J.* **15**, 6069–6074.

13. Ruff, C., Furch, M., Brenner, B., Manstein, D. J. & Meyhofer, E. (2001). Single-molecule tracking of myosins with genetically engineered amplifier domains. *Nat. Struct. Biol.* **8**, 226–229.

14. Okten, Z., Churchman, L. S., Rock, R. S. & Spudich, J. A. (2004). Myosin VI walks hand-over-hand along actin. *Nat. Struct. Mol. Biol.* **11**, 884–887.

15. Sweeney, H. L., Park, H., Zong, A. B., Yang, Z., Selvin, P. R. & Rosenfeld, S. S. (2007). How myosin VI coordinates its heads during processive movement. *EMBO J.* **26**, 2682–2692.

16. Kliche, W., Fujita-Becker, S., Kollmar, M., Manstein, D. J. & Kull, F. J. (2001). Structure of a genetically engineered molecular motor. *EMBO J.* **20**, 40–46.

17. O'Connell, C. B. & Mooseker, M. S. (2003). Native myosin-IXb is a plus-, not a minus-end-directed motor. *Nat. Cell Biol.* **5**, 171–172.

18. Sun, Y., Schroeder, H. W., 3rd, Beausang, J. F., Homma, K., Ikebe, M. & Goldman, Y. E. (2007). Myosin VI walks "wiggly" on actin with large and variable tilting. *Mol. Cell*, **28**, 954–964.

19. Veigel, C., Wang, F., Bartoo, M. L., Sellers, J. R. & Molloy, J. E. (2002). The gated gait of the processive molecular motor, myosin V. *Nat. Cell Biol.* **4**, 59–65.

20. Lan, G. & Sun, S. X. (2006). Flexible light-chain and helical structure of F-actin explain the movement and step size of myosin-VI. *Biophys. J.* **91**, 4002–4013.

21. Chevalier, B. S., Kortemme, T., Chadsey, M. S., Baker, D., Monnat, R. J. & Stoddard, B. L. (2002). Design, activity, and structure of a highly specific artificial endonuclease. *Mol. Cell*, **10**, 895–905.